SUPPORTING INFORMATION

Corona Exchange Dynamics on Carbon Nanotubes by Multiplexed Fluorescence Monitoring

Rebecca L. Pinals,[a,‡] Darwin Yang,[a,‡] Alison Lui,[a] Wendy Cao,[b] and Markita P. Landry*[,a,c,d,e]

[a] Department of Chemical and Biomolecular Engineering, University of California, Berkeley, Berkeley, California 94720, United States

[b] Department of Chemistry, University of California, Berkeley, Berkeley, California 94720, United States

[c] Innovative Genomics Institute (IGI), Berkeley, California 94720, United States

[d] California Institute for Quantitative Biosciences, QB3, University of California, Berkeley, Berkeley, California 94720, United States

[e] Chan-Zuckerberg Biohub, San Francisco, California 94158, United States

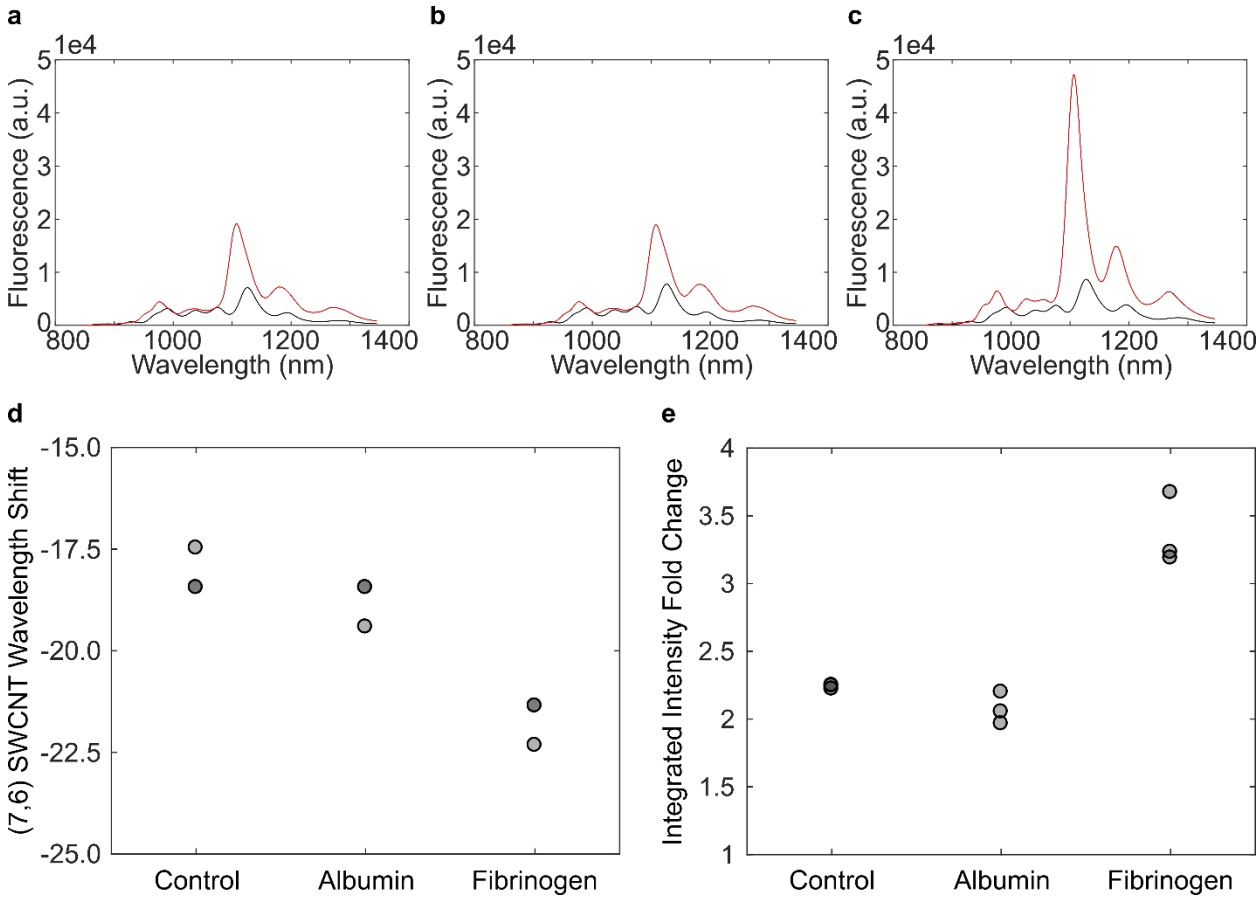

Figure S1. Surfactant-induced fluorescence change of ssDNA-SWCNTs incubated with protein. Near-infrared (nIR) spectra of 5 µg/mL $(GT)_6$-SWCNTs before (black) and after (red) addition of 0.5% (w/v) SDBS. (b-c) nIR spectra of 5 µg/mL $(GT)_6$-SWCNTs incubated with 40 µg/mL (b) albumin or (c) fibrinogen for 40 min before (black) and after (red) addition of 0.5% (w/v) SDBS. Change in (d) (7,6) SWCNT wavelength of peak emission and (e) integrated fluorescence intensity (800-1400 nm) observed 1 min after addition of SDBS (N = 3). Nanosensor excitation was with 721 nm light.

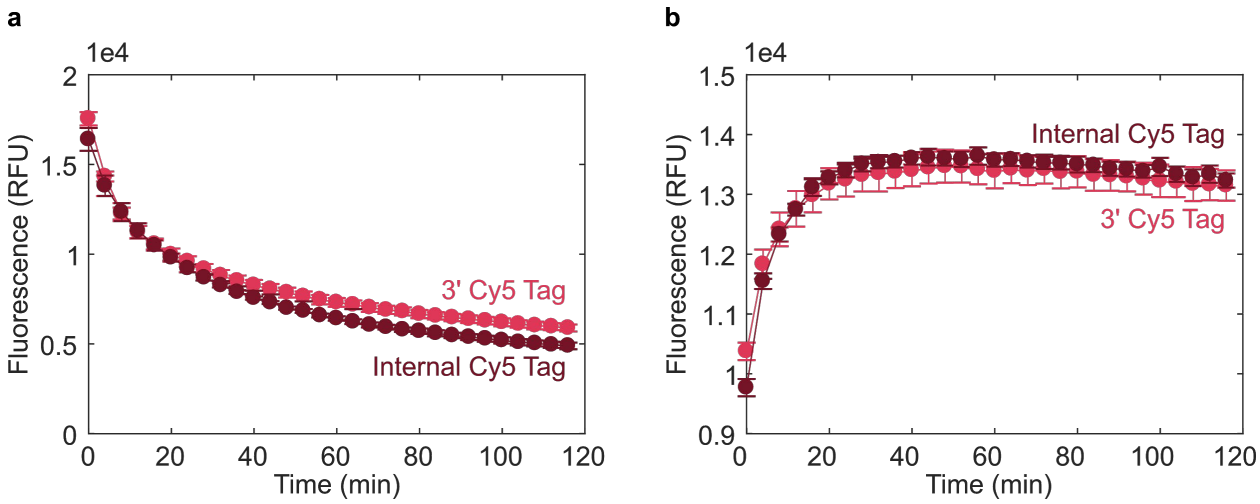

Figure S2. Effect of Cy5 tag location on ssDNA adsorption and protein-induced desorption. (a) Cy5 fluorescence tracking of 0.4 µM 3'- or internal-Cy5 tagged $(GT)_6$ ssDNA added to 5 µg/mL unlabeled $(GT)_6$-SWCNT. (b) Cy5 fluorescence tracking upon addition of 160 µg/mL fibrinogen, 3 h post-incubation with $(GT)_6$-Cy5. Error bars represent standard error between experimental replicates (N = 3).

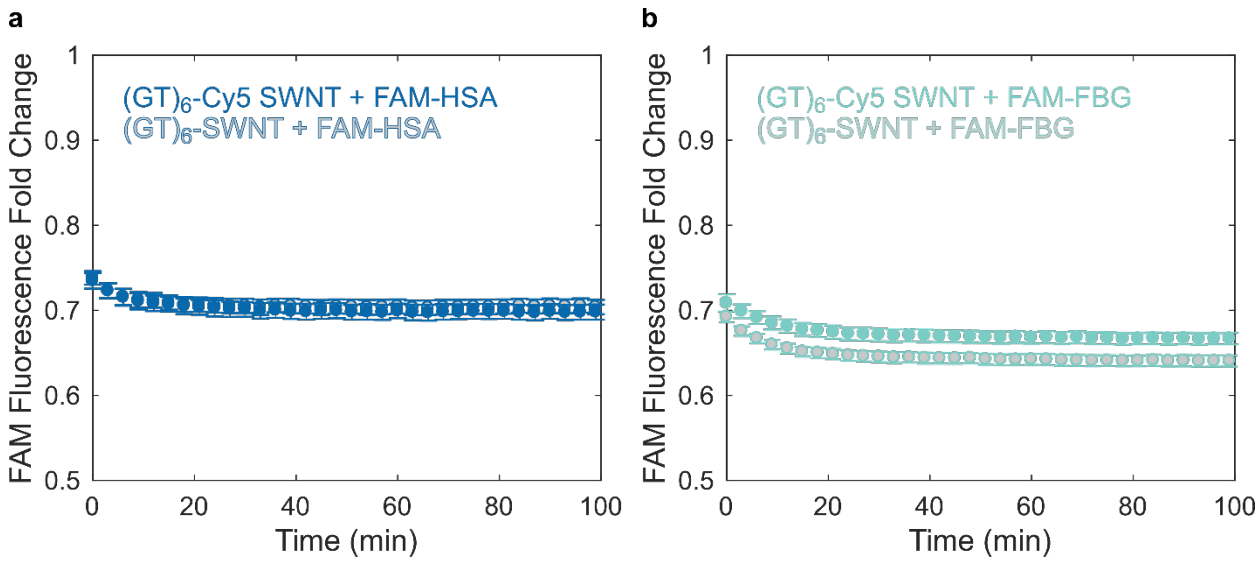

Figure S3. Effect of Cy5 ssDNA tag on protein adsorption. Quenching of FAM-protein upon addition of 40 µg/mL (a) FAM-HSA or (b) FAM-FBG to 5 µg/mL $(GT)_6$-Cy5-SWCNTs or $(GT)_6$-SWCNTs. Error bars represent standard error between experimental replicates (N = 3).

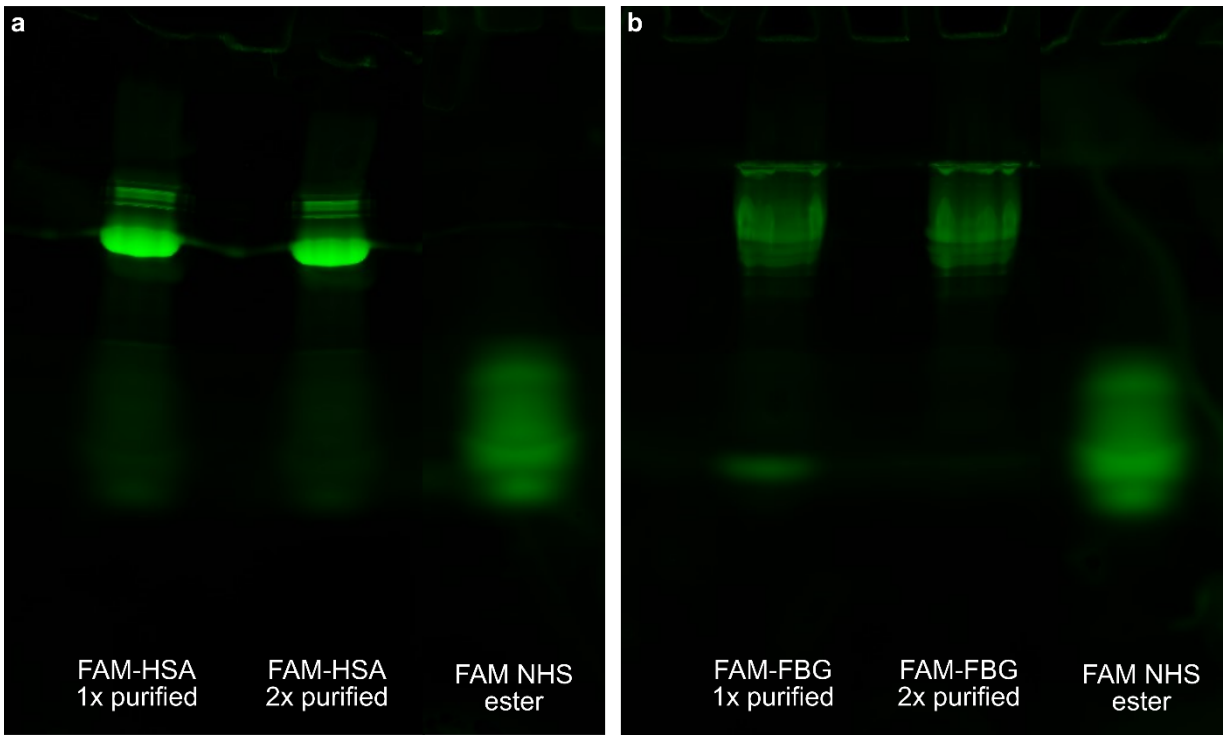

Figure S4. Polyacrylamide gel electrophoresis (PAGE) to quantify purification of labeled FAM-protein solutions. 12% acrylamide (total monomer) gel images of FAM-labeled (a) albumin (FAM-HSA) and (b) fibrinogen (FAM-FBG) post-purification to assess amount of free FAM remaining.

Table S1. Quantification of free FAM remaining in labeled FAM-protein solutions. Molar percentages of FAM-protein and free FAM are calculated based on gel band intensity and protein degree of labeling for (a) FAM-HSA and (b) FAM-FBG.

a

Sample	Band ID	Mole %
FAM-HSA, 1x pure	FAM-Protein	69.7%
	FAM	30.3%
FAM-HSA, 2x pure	FAM-Protein	67.8%
	FAM	32.2%
FAM	FAM	100.0%

b

Sample	Band ID	Mole %
FAM-FBG, 1x pure	FAM-Protein	70.5%
	FAM	29.5%
FAM-FBG, 2x pure	FAM-Protein	86.2%
	FAM	13.8%
FAM	FAM	100.0%

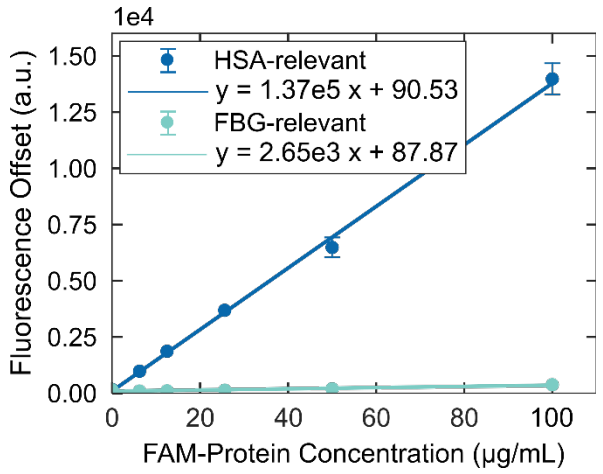

Figure S5. Fluorescence offset due to free FAM binding to SWCNT surface. FAM NHS ester was injected into solution with or without SWCNTs to quantify free fluorophore binding to the SWCNT. Free FAM concentrations tested were calculated based on molar percentage of free fluorophore at FAM-HSA or FAM-FBG concentrations between 0 and 100 µg/mL. Fluorescence offset was calculated as the difference between FAM fluorescence in the presence and absence SWCNTs. Offset is incorporated for all data conversion from fluorescence to concentration. Error bars represent standard deviation between technical replicates (N = 3).

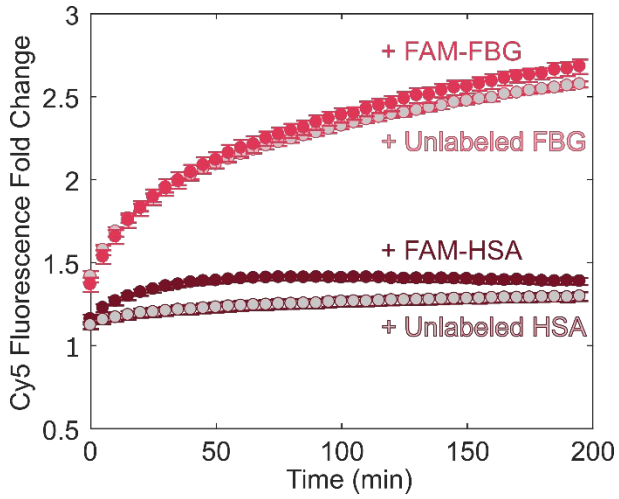

Figure S6. Desorption of ssDNA-Cy5 from SWCNT induced by FAM-labeled vs unlabeled protein. Dequenching of $(GT)_6$-Cy5 due to desorption from SWCNT upon addition of 40 µg/mL FAM-protein or unlabeled protein. Error bars represent standard error between experimental replicates (N = 3).

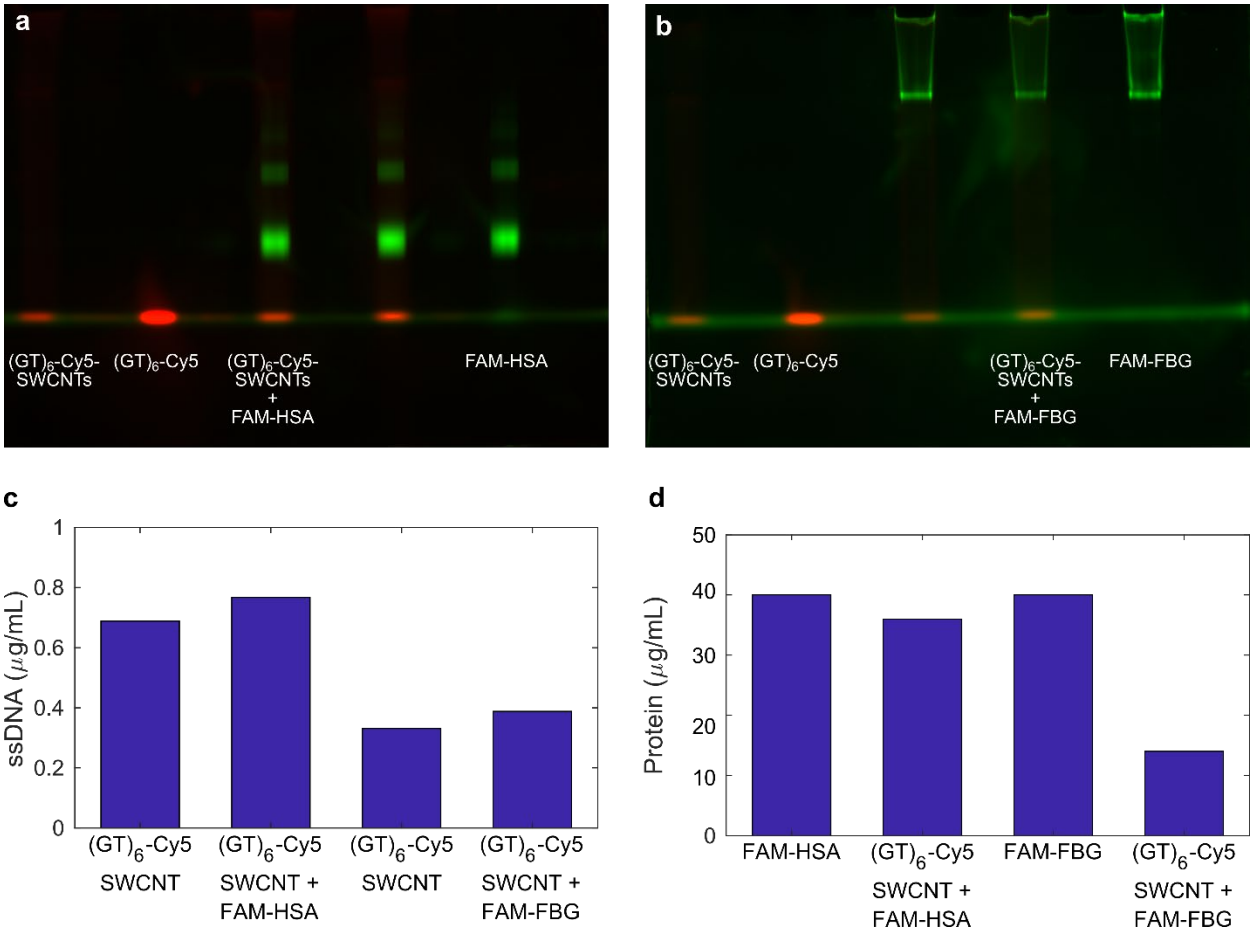

Figure S7. Native polyacrylamide gel electrophoresis (PAGE) to quantify ssDNA and protein exchange. Incubation of (a) FAM-HSA or (b) FAM-FBG proteins with $(GT)_6$-Cy5-SWCNTs for 1 h (final concentrations 5 μg/mL of $(GT)_6$-Cy5-SWCNTs with 40 μg/mL of either FAM-HSA or FAM-FBG). Quantification of concentration via fluorescence for (c) Cy5 bands (red) and (d) FAM bands (green).

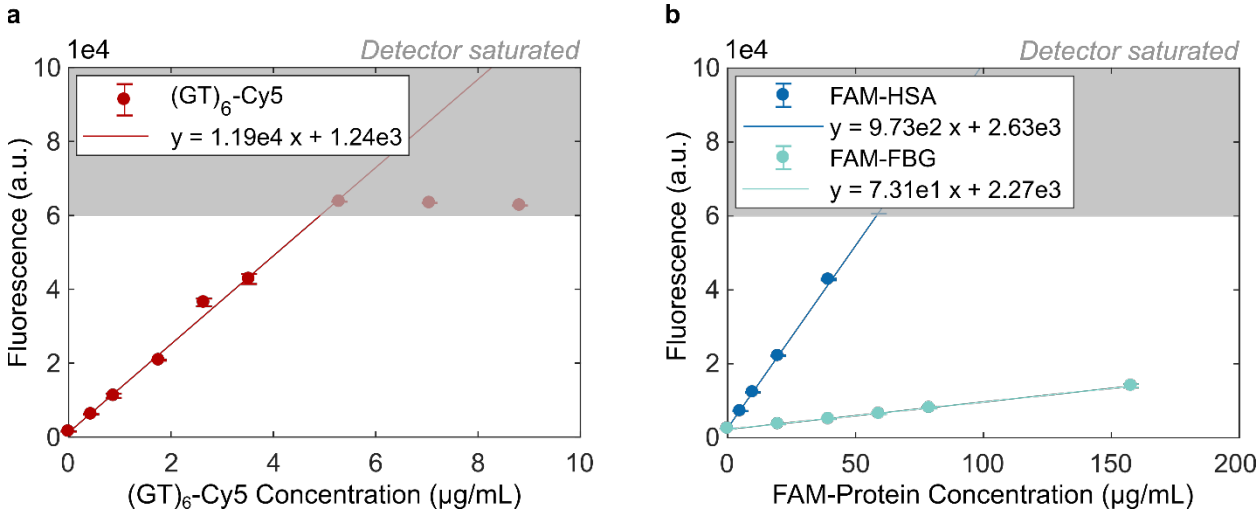

Figure S8. Conversion of fluorescence to concentration. Standard curves correlating fluorescence to fluorophore-labeled entity concentration for (a) Cy5-labeled $(GT)_6$ and (b) FAM-labeled proteins, FAM-HSA and FAM-FBG. Error bars represent standard deviation between technical replicates (N = 3).

Table S2. Full kinetic model fit parameters and mean relative errors (MREs).

Protein	Concentration (μg/mL)	k_1 (mL μg^{-1} s^{-1})	k_2 (s^{-1})	k_3 (mL μg^{-1} s^{-1})	k_4 (s^{-1})	$[*]_T$ (μg mL^{-1})	MRE protein	MRE ssDNA
Albumin	5	1.54E-06	8.40E-06	9.44E-06	5.9E-03	364.60	1.21%	0.25%
	10	1.41E-06	1.18E-05	7.86E-06	8.1E-03	525.60	0.83%	0.90%
	40	1.10E-06	1.34E-05	8.87E-06	1.1E-02	514.26	0.35%	3.01%
	60	1.22E-06	2.07E-05	9.34E-06	1.2E-02	483.76	0.41%	2.53%
Fibrinogen	40	1.15E-06	4.27E-05	1.38E-05	2.6E-03	619.82	4.71%	2.96%
	60	2.18E-06	6.64E-05	1.69E-05	3.7E-03	485.72	2.98%	3.47%
	80	2.09E-06	7.65E-05	1.48E-05	5.4E-03	562.90	1.37%	4.14%
	160	2.30E-06	9.09E-05	1.18E-05	9.2E-03	617.74	0.74%	4.74%

Table S3. Sensitivity analysis in kinetic fitting and resultant optimized initial conditions.

	k_1 (mL μg^{-1} s^{-1})	k_2 (s^{-1})	k_3 (mL μg^{-1} s^{-1})	k_4 (s^{-1})	$[*]_T$ (μg mL^{-1})
Range of Initial Conditions Tested	1.0E-03	1.0E-02	1.0E-03	1.0	1000
	1.0E-04	1.0E-03	1.0E-04	0.1	100
	1.0E-05				
Albumin Optimized Initial Conditions	1.0E-04	1.0E-02	1.0E-03	1.0	100
Fibrinogen Optimized Initial Conditions	1.0E-04	1.0E-02	1.0E-04	0.1	100

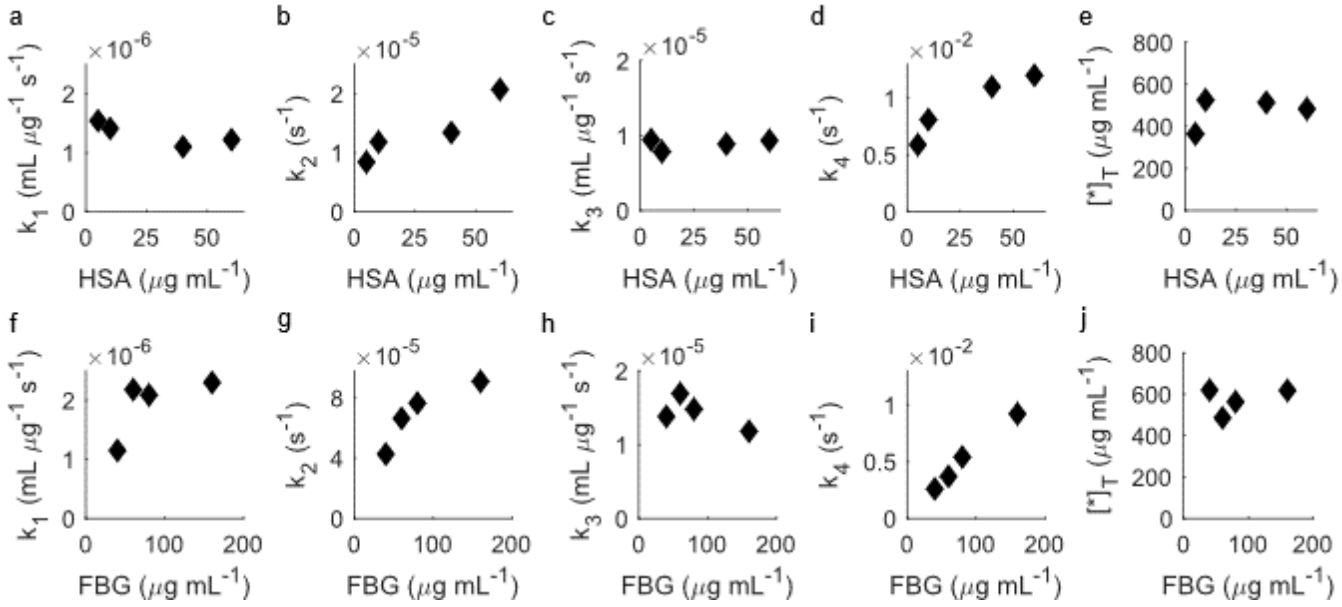

Figure S9. Full kinetic model fit parameters as functions of added protein concentrations. Fit parameters of (a) k_1 (ssDNA adsorption rate constant), (b) k_2 (ssDNA desorption rate constant), (c) k_3 (protein adsorption rate constant), (d) k_4 (protein desorption rate constant), and (e) $[*]_T$ (total SWCNT surface site concentration) for HSA in the top row and (f-j) the respective values for FBG in the bottom row.

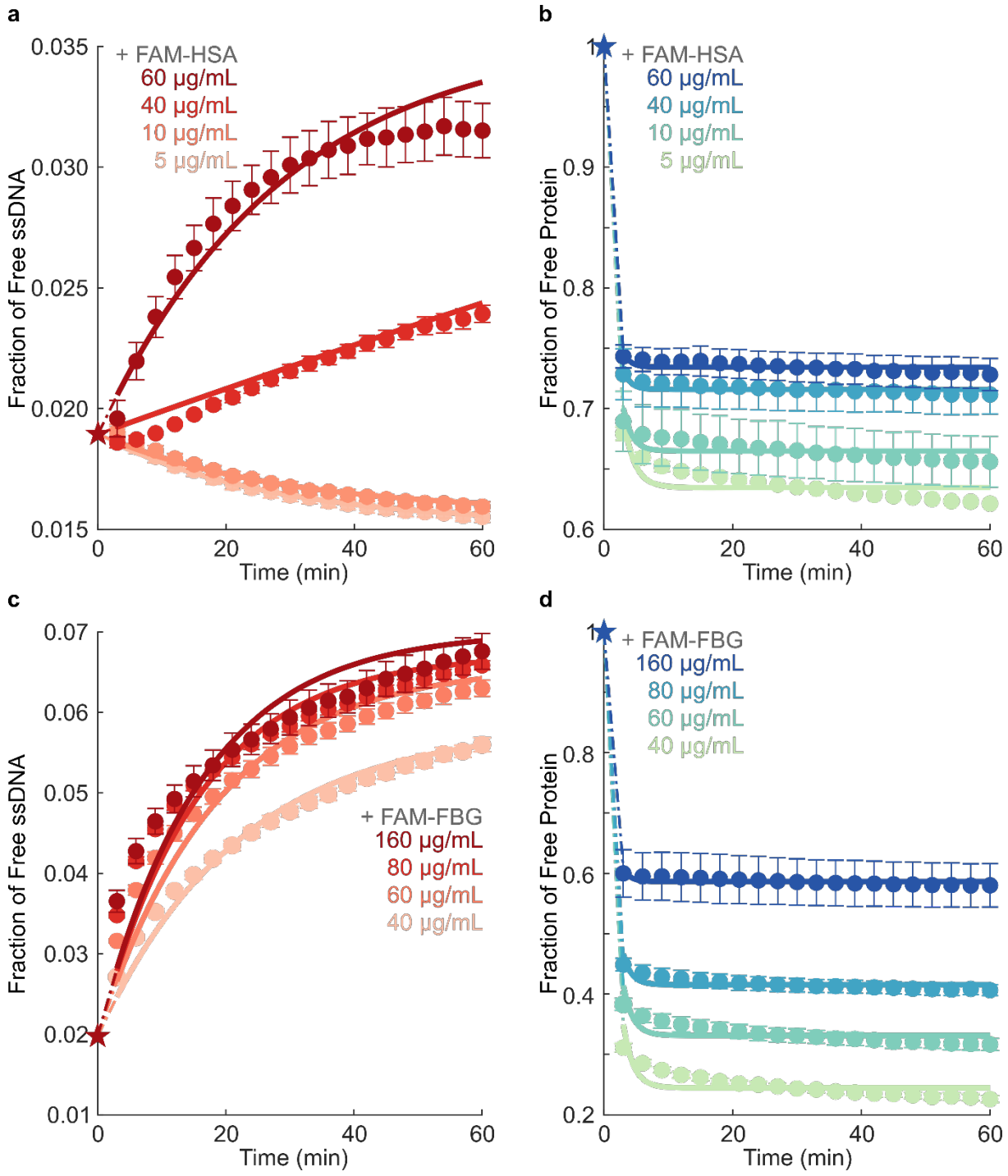

Figure S10. Kinetic model of competitive exchange between ssDNA and protein on SWCNTs fit to fluorescence data to extract rate constants, with constrained SWCNT surface site concentration. Fraction of (a) $(GT)_6$-Cy5 ssDNA and (b) FAM-labeled albumin (FAM-HSA) protein free in solution for varying concentrations of FAM-HSA injected into 5 µg/mL $(GT)_6$-Cy5-SWCNT solution. Fraction of (c) $(GT)_6$-Cy5 ssDNA and (d) FAM-labeled fibrinogen (FAM-FBG) protein free in solution for varying concentrations of FAM-FBG injected into $(GT)_6$-Cy5-SWCNT solution. Star data points represent initial conditions used for solving model differential equations. Curves were fit with constrained $[*]_T$ per protein. Error bars represent standard error between experimental replicates (N = 3).

Table S4. Full kinetic model fit parameters and mean relative errors (MREs) for fitting with constrained SWCNT surface site concentration.

Protein	Concentration (µg/mL)	k_1 (mL µg^{-1} s^{-1})	k_2 (s^{-1})	k_3 (mL µg^{-1} s^{-1})	k_4 (s^{-1})	$[*]_T$ (µg mL^{-1})	MRE protein	MRE ssDNA
Albumin	5	1.47E-06	9.58E-06	8.74E-06	6.41E-03	429.69	1.24%	0.37%
	10	1.38E-06	9.25E-06	9.92E-06	8.29E-03		0.84%	0.63%
	40	6.93E-08	2.18E-06	1.06E-05	1.11E-02		0.35%	1.83%
	60	1.35E-06	2.04E-05	1.06E-05	1.19E-02		0.41%	2.66%
Fibrinogen	40	8.51E-07	4.41E-05	9.73E-06	2.64E-03	871.49	4.76%	2.52%
	60	1.01E-06	5.91E-05	9.14E-06	3.74E-03		3.00%	4.06%
	80	1.19E-06	7.04E-05	9.34E-06	5.43E-03		1.38%	4.46%
	160	1.20E-06	7.22E-05	7.96E-06	9.03E-03		0.74%	5.64%

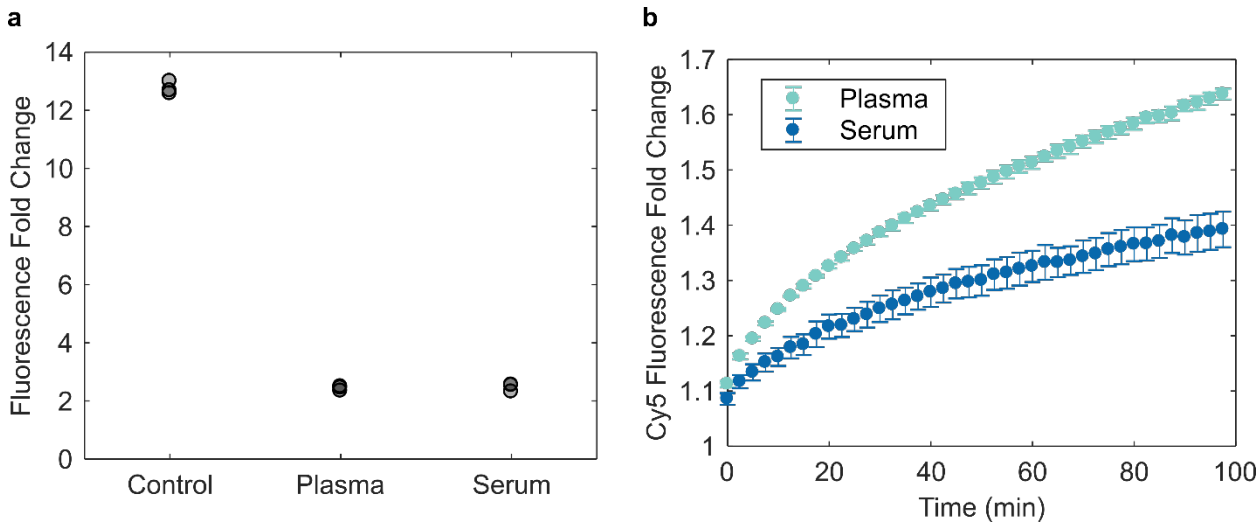

Figure S11. Comparison of plasma- vs serum-induced effects on ssDNA-SWCNTs. (a) Change in 1200 nm fluorescence intensity of 5 µg/mL $(GT)_6$-SWCNTs, pre-incubated for 40 min with PBS, plasma, or serum normalized to 40 µg/mL total protein concentration, before and after addition of 200 µM dopamine (N = 3). Nanosensor excitation was with 721 nm light. (b) $(GT)_6$-Cy5 fluorescence fold change upon desorption from 5 µg/mL SWCNTs induced by addition of plasma or serum, 40 µg/mL total protein concentration. Error bars represent standard error between experimental replicates (N = 3).

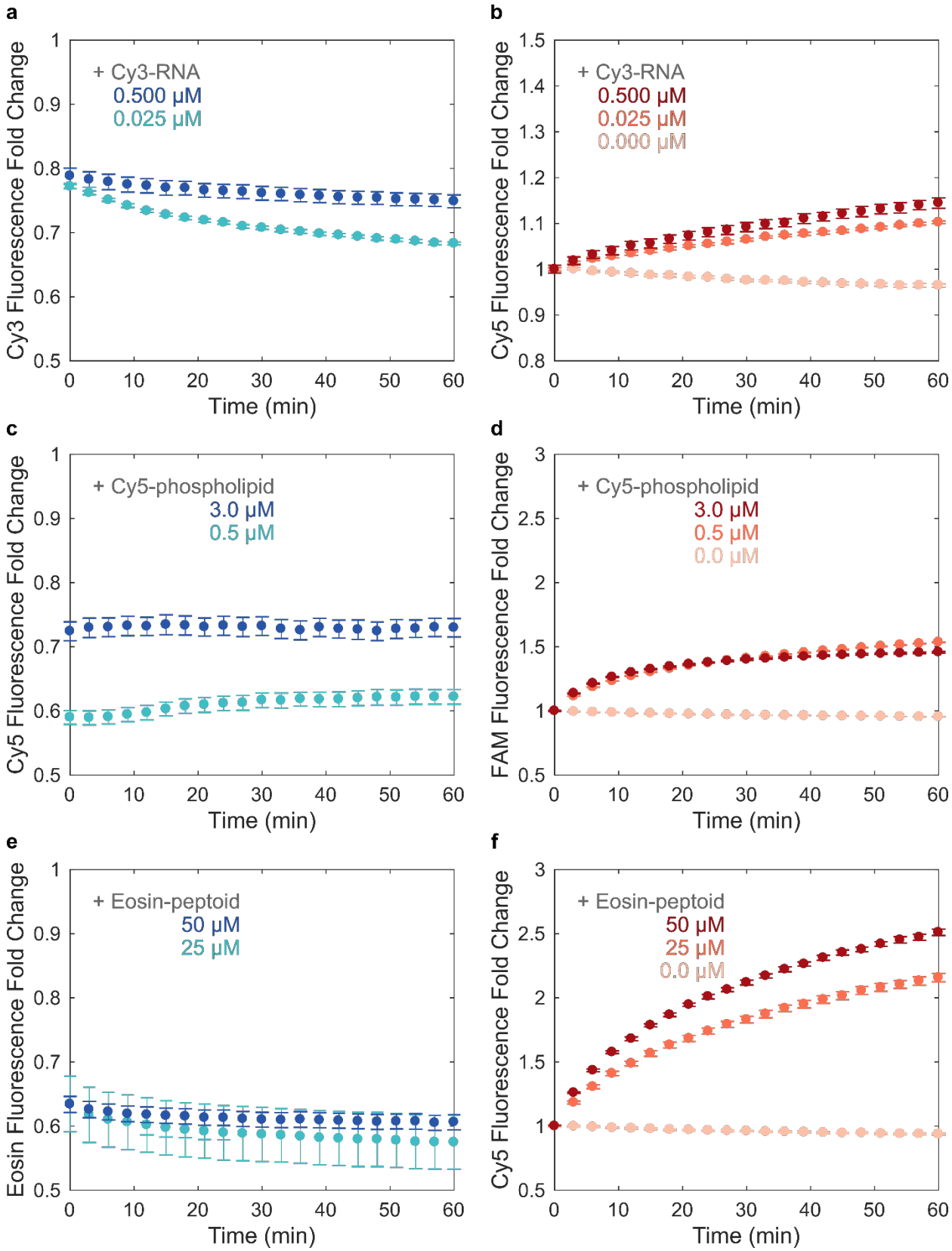

Figure S12. Adsorption of various fluorophore-tagged biomolecular species to ssDNA-SWCNTs. Adsorption of varying concentrations of biomolecules (as listed in figure) to 5 μg/mL $(GT)_6$-SWCNTs. (Column 1) Quenching of fluorophore-tagged biomolecules adsorbing to $(GT)_6$-SWCNTs: (a) Cy3-RNA, (c) Cy5-phospholipid (DSPE-PEG(2000)-N-Cy5), and (e) eosin-peptoid ($(Nae–Npe)_9$-$(Nce–Npe)_9$). (Column 2) Corresponding dequenching of fluorophore-tagged $(GT)_6$ ssDNA desorbing from SWCNT surface: (b) $(GT)_6$-Cy5, (d) $(GT)_6$-FAM, and (f) $(GT)_6$-Cy5. Error bars represent standard error between experimental replicates (N = 3).

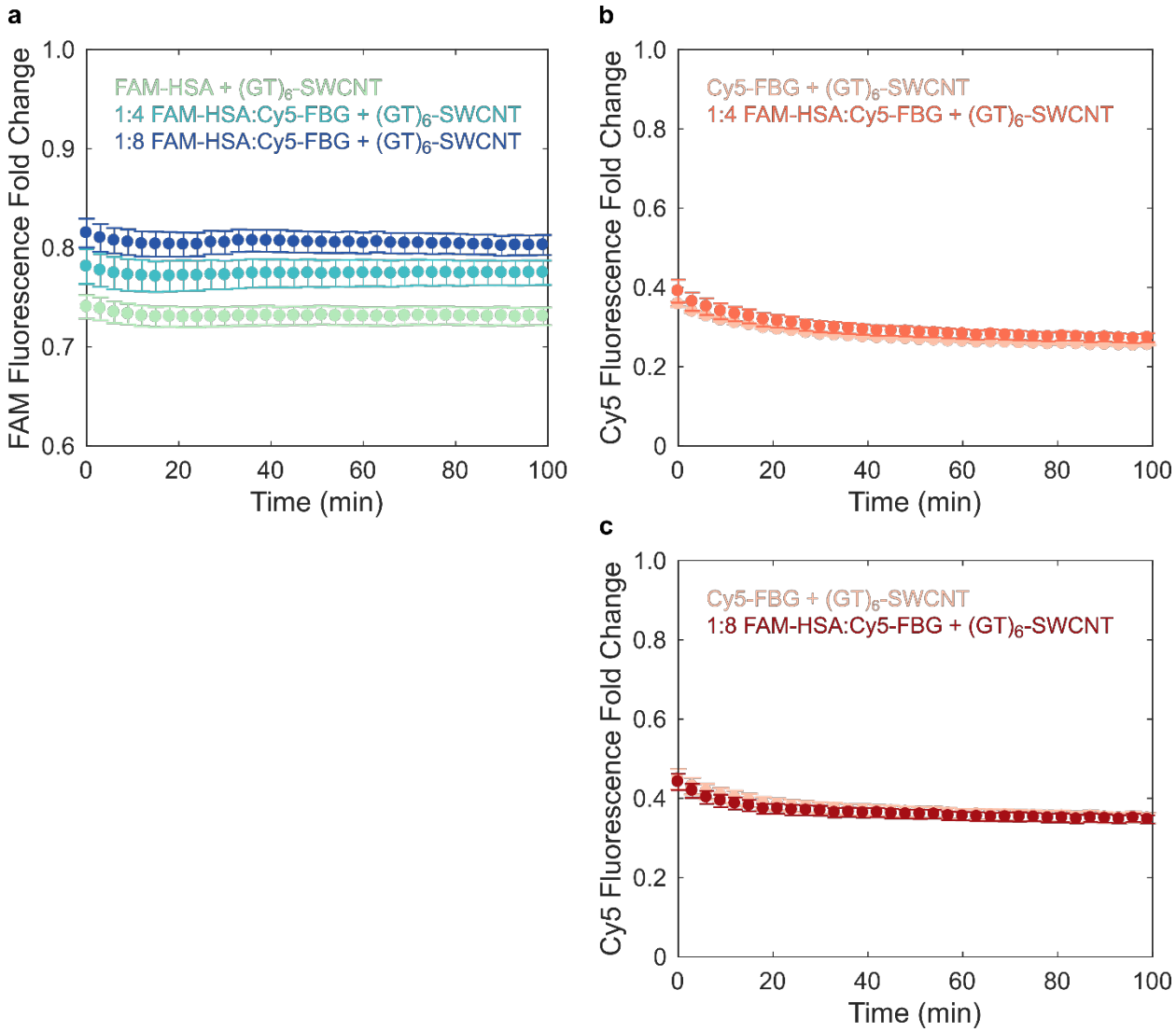

Figure S13. Tracking competitive adsorption of two protein species onto SWCNT surface. (a) Adsorption of 20 µg/mL FAM-HSA to 5 µg/mL $(GT)_6$ SWCNTs tracked by FAM quenching in the presence of Cy5-conjugated FBG at 0, 80, and 160 µg/mL. (b-c) Comparison of Cy5-FBG adsorption in the presence and absence of 20 µg/mL FAM-HSA, with Cy5-FBG concentrations of (b) 80 µg/mL and (c) 160 µg/mL. Error bars represent standard error between experimental replicates (N = 3).

SI MATERIALS AND METHODS

S.1. PAGE to quantify ssDNA and protein exchange

To validate the corona exchange assay, we performed polyacrylamide gel electrophoresis (PAGE) to quantify the unbound DNA and protein after 1-h incubation period of $(GT)_6$-Cy5-SWCNTs with either FAM-labeled human serum albumin (HSA) or fibrinogen (FBG) proteins. FAM-proteins were incubated with $(GT)_6$-Cy5-SWCNTs (final concentrations of 5 μg/mL of $(GT)_6$-Cy5-SWCNT with 40 μg/mL of either FAM-HSA or FAM-FBG) for 1 h, then free protein and ssDNA were quantified by PAGE run according to the Ornstein-Davis protocol[1] (adapted in Bio-Rad Mini-PROTEAN Tetra Cell manual). Samples were added to PAGE sample buffer (0.0625 M Tris-HCl, 30% glycerol) in a 1:2 ratio of sample to buffer. 20 μL total sample volume was applied per well. PAGE separation was carried out in 1 mm vertical mini gel format (Bio-Rad Mini-PROTEAN Tetra Cell) with a discontinuous buffer system under native conditions. Gel composition was 8% acrylamide (total monomer), 0.375 M Tris-HCl, 0.05% APS, 0.05% TEMED for the resolving gel and 4% acrylamide (total monomer), 0.125 M Tris-HCl, 0.05% APS, 0.1% TEMED for the stacking gel. Electrode buffer was 25 mM Tris and 192 mM glycine (pH 8.3). Separation was run with 200 V for 30 min, gels were extracted, and the FAM and Cy5 labels were visualized with a gel imager (Typhoon FLA 9500, 473 nm and 635 nm lasers for FAM and Cy5, respectively, General Electric) (Figure S7). FAM and Cy5 fluorescence intensities were quantified with ImageJ. Control PAGE experiments were done to validate that (i) all bands are resolvable on separate color channels and (ii) there are negligible interactions between proteins and ssDNA. The band structure for HSA run on native PAGE was confirmed by previous literature,[2–4] therefore HSA bands were quantified by summing the 3 bands. FBG was quantified by the sole band that entered the gel. The uniform lower green band is accounted for by diffusion of the small free FAM molecule across the wells upon sample loading and prior to electric field turn-on (as confirmed by control gels).

S.2. Biomolecule corona exchange assay

Cy3-RNA: UUC CGU AUG UUG CAU CAC CTT (5' Cy3-labeled custom RNA oligo with HPLC purification, Integrated DNA Technologies, Inc.). This particular RNA sequence was chosen because it serves as the antisense strand in a SWCNT-mediated plant delivery study.[5] Exchange was monitored with $(GT)_6$-Cy5-SWCNTs.

Cy5-phospholipid: 1,2-distearoyl-sn-glycero-3-phosphoethanolamine-N-[amino(polyethylene glycol)-2000]-N-(Cyanine 5), abbreviated DSPE-PEG(2000)-N-Cy5 (Avanti Polar Lipids, Inc.). This phospholipid was chosen because it has been previously used to functionalize SWCNT for brain imaging applications.[6] Exchange was monitored with $(GT)_6$-FAM-SWCNTs.

Eosin-peptoid: $(Nae–Npe)_9$-$(Nce–Npe)_9$): N-(2-aminoethyl) glycine (Nae) and N-(2-phenethyl) glycine (Npe) units, abbreviated $(Nae–Npe)_9$, and N-(2-carboxyethyl) glycine (Nce) and Npe, abbreviated $(Nce–Npe)_9$.[7] This peptoid sequence was chosen because it has been used to construct a SWCNT-based nanosensor.[8] Exchange was monitored with $(GT)_6$-Cy5-SWCNTs.

SI CALCULATIONS

S.3. Calculation of ssDNA-protein exchange energies on SWCNTs

Calculation of ssDNA-SWCNT binding energy

For this analysis, we use adsorption energies of nucleotides to SWCNTs from Johnson et al.'s solvent-explicit, all-atom MD simulations of nucleotide hetero- and homo-polymers to SWCNTs.[9] Individual nucleotide energies (Table S5) are used to calculate the total binding energy of $(GT)_6$ ssDNA to SWCNTs as **-166.0 kcal/mol**. This total energy of $(GT)_6$-SWCNT binding is in close agreement with values calculated from other sources by various methods: (i) Das et al.,[10] calculated from density functional theory (DFT) and experimentally from isothermal titration calorimetry (ITC) (-149.4 kcal/mol) and (ii) Gowtham et al.,[11] calculated from a first principles model (-114.8 kcal/mol) (Table S5).

Table S5. Adsorption energies of individual nucleotide to SWCNTs.

Nucleotide	Energy (kcal/mol)[9]	Energy (kcal/mol)[10]	Energy (kcal/mol)[11]
A	-13.84	-11.30	-8.994
G	-14.99	-13.14	-11.30
C	-11.07	-6.918	-6.688
T	-12.68	-11.76	-7.841
$(GT)_6$	-166.0	-149.4	-114.8

Calculation of protein-SWCNT binding energy

For the analogous protein-SWCNT binding energies, we use an approximate value of -10 kcal/mol per amino acid residue based on the following studies: (i) Shen et al.[12] performed solvent-explicit MD simulations of human serum albumin (HSA) helices on SWCNTs, with an average of -13.51 kcal/mol per residue and (ii) DFT calculations of aromatic acids on SWCNTs reveal an average energy of ~-10 kcal/mol per residue.[13,14]

Exchange of ssDNA and protein on SWCNT

We analyze the exchange of $(GT)_6$ ssDNA, originally adsorbed on the SWCNT surface, to protein that will adsorb to an equivalent surface area on the SWCNT. The contact area of $(GT)_6$ on SWCNTs has been previously determined by our lab via MD simulations as **2800 Å²**.[15] As an estimate for how many amino acid residues would occupy this same surface area, we use dimensions for protein beta sheets as a proxy for peptides adsorbing to SWCNTs. Lengthwise, beta sheet spacing is 3.25 Å per residue, therefore *X* residues occupy a length of 3.25**X* Å. The lateral dimension is approximated as twice the residue's variable R-group dimension, based on beta sheet geometry. Assuming aromatic residues primarily interact with SWCNTs (as determined previously in literature[13,14,16] as well as our lab's protein corona compositional studies), the average R-group lateral dimension is 5.69 Å, so 2*5.69 = 11.38 Å. Thus, contact area per residue is $SA_{residue}$ = (3.25**X* Å)*(11.38 Å) = 36.99**X* Å². For the $(GT)_6$ surface area of 2800 Å², this translates to 75.71 amino acids occupying the same surface area on the SWCNT surface. Thus, the total binding energy of protein to SWCNTs is 75.71*-10 kcal/mol = **-757.1 kcal/mol**. This is in order-of-magnitude agreement with Lu et al.'s[17] MD simulation of HSA adsorption to carboxylated-SWCNTs, with total energy ~-500 kcal/mol.

We assume independent binding of ssDNA and protein to the SWCNT surface, as done with the corona exchange kinetic model. This assumption is also in agreement with the literature values, where the "initial" state is the SWCNT in solvent and the "final" state is bound ssDNA or protein to SWCNTs. We note that it is energetically unfavorable to expose the hydrophobic SWCNT surface to solvent, accounting for a *positive* unbinding energy (unfavorable; ssDNA removed from SWCNT surface) and a corresponding *negative* binding energy (favorable; protein added to SWCNT surface). Finally, the Gibbs free energy of exchange from ssDNA to protein on the SWCNT surface can be written as:

$$\Delta G_{exchange} = \Delta G_{protein-SWCNT} + \Delta G_{ssDNA-SWCNT}$$

$$\Delta G_{exchange} = \left(-757.1\ \frac{kcal}{mol}\right) + \left(+166.0\frac{kcal}{mol}\right) = \mathbf{-591.0\ \frac{kcal}{mol}}$$

This analysis emphasizes the energetically favorable displacement of ssDNA on the SWCNT surface by replacement with protein adsorption. This negative net change in free energy in favor of protein-SWCNT binding over ssDNA-SWCNT binding holds across a range of previously reported literature values.

REFERENCES

(1) Ornstein, L. Disc Electrophoresis-I Background and Theory*. *Annals of the New York Academy of Sciences* **1964**, *121* (2), 321–349. https://doi.org/10.1111/j.1749-6632.1964.tb14207.x.

(2) Braz, V. A.; Howard, K. J. Separation of Protein Oligomers by Blue Native Gel Electrophoresis. *Anal Biochem* **2009**, *388* (1), 170–172. https://doi.org/10.1016/j.ab.2009.02.019.

(3) Peters, T. Serum Albumin. In *Advances in Protein Chemistry*; Anfinsen, C. B., Edsall, J. T., Richards, F. M., Eds.; Academic Press, 1985; Vol. 37, pp 161–245. https://doi.org/10.1016/S0065-3233(08)60065-0.

(4) Carter, D. C.; Ho, J. X. Structure of Serum Albumin. In *Advances in Protein Chemistry*; Anfinsen, C. B., Edsall, J. T., Richards, F. M., Eisenberg, D. S., Eds.; Lipoproteins, Apolipoproteins, and Lipases; Academic Press, 1994; Vol. 45, pp 153–203. https://doi.org/10.1016/S0065-3233(08)60640-3.

(5) Demirer, G. S.; Zhang, H.; Goh, N. S.; Chang, R.; Landry, M. P. Nanotubes Effectively Deliver SiRNA to Intact Plant Cells and Protect SiRNA against Nuclease Degradation. *bioRxiv* **2019**, 564427. https://doi.org/10.1101/564427.

(6) Godin, A. G.; Varela, J. A.; Gao, Z.; Danné, N.; Dupuis, J. P.; Lounis, B.; Groc, L.; Cognet, L. Single-Nanotube Tracking Reveals the Nanoscale Organization of the Extracellular Space in the Live Brain. *Nature Nanotechnology* **2016**, *12* (3), 238–243. https://doi.org/10.1038/nnano.2016.248.

(7) Nam, K. T.; Shelby, S. A.; Choi, P. H.; Marciel, A. B.; Chen, R.; Tan, L.; Chu, T. K.; Mesch, R. A.; Lee, B.-C.; Connolly, M. D.; et al. Free-Floating Ultrathin Two-Dimensional Crystals from Sequence-Specific Peptoid Polymers. *Nature Materials* **2010**, *9* (5), 454–460. https://doi.org/10.1038/nmat2742.

(8) Chio, L.; Yang, D.; Landry, M. Surface Engineering of Nanoparticles to Create Synthetic Antibodies. In *Synthetic Antibodies*; Methods in Molecular Biology; Humana Press, New York, NY, 2017; pp 363–380. https://doi.org/10.1007/978-1-4939-6857-2_23.

(9) Johnson, R. R.; Johnson, A. T. C.; Klein, M. L. Probing the Structure of DNA−Carbon Nanotube Hybrids with Molecular Dynamics. *Nano Lett.* **2008**, *8* (1), 69–75. https://doi.org/10.1021/nl071909j.

(10) Das, A.; Sood, A. K.; Maiti, P. K.; Das, M.; Varadarajan, R.; Rao, C. N. R. Binding of Nucleobases with Single-Walled Carbon Nanotubes: Theory and Experiment. *Chemical Physics Letters* **2008**, *453* (4), 266–273. https://doi.org/10.1016/j.cplett.2008.01.057.

(11) Gowtham, S.; Scheicher, R. H.; Pandey, R.; Karna, S. P.; Ahuja, R. First-Principles Study of Physisorption of Nucleic Acid Bases on Small-Diameter Carbon Nanotubes. *Nanotechnology* **2008**, *19* (12), 125701. https://doi.org/10.1088/0957-4484/19/12/125701.

(12) Shen, J.-W.; Wu, T.; Wang, Q.; Kang, Y. Induced Stepwise Conformational Change of Human Serum Albumin on Carbon Nanotube Surfaces. *Biomaterials* **2008**, *29* (28), 3847–3855. https://doi.org/10.1016/j.biomaterials.2008.06.013.

(13) Yang, Z.; Wang, Z.; Tian, X.; Xiu, P.; Zhou, R. Amino Acid Analogues Bind to Carbon Nanotube via π-π Interactions: Comparison of Molecular Mechanical and Quantum Mechanical Calculations. *J. Chem. Phys.* **2012**, *136* (2), 025103. https://doi.org/10.1063/1.3675486.

(14) Rajesh, C.; Majumder, C.; Mizuseki, H.; Kawazoe, Y. A Theoretical Study on the Interaction of Aromatic Amino Acids with Graphene and Single Walled Carbon Nanotube. *J. Chem. Phys.* **2009**, *130* (12), 124911. https://doi.org/10.1063/1.3079096.

(15) Beyene, A. G.; Alizadehmojarad, A. A.; Dorlhiac, G.; Goh, N.; Streets, A. M.; Král, P.; Vuković, L.; Landry, M. P. Ultralarge Modulation of Fluorescence by Neuromodulators in Carbon Nanotubes Functionalized with Self-Assembled Oligonucleotide Rings. *Nano Lett.* **2018**, *18* (11), 6995–7003. https://doi.org/10.1021/acs.nanolett.8b02937.

(16) Wang, S.; Humphreys, E. S.; Chung, S.-Y.; Delduco, D. F.; Lustig, S. R.; Wang, H.; Parker, K. N.; Rizzo, N. W.; Subramoney, S.; Chiang, Y.-M.; et al. Peptides with Selective Affinity for Carbon Nanotubes. *Nature Mater* **2003**, *2* (3), 196–200. https://doi.org/10.1038/nmat833.

(17) Lu, N.; Sui, Y.; Ding, Y.; Tian, R.; Li, L.; Liu, F. Adsorption of Human Serum Albumin on Functionalized Single-Walled Carbon Nanotubes Reduced Cytotoxicity. *Chemico-Biological Interactions* **2018**. https://doi.org/10.1016/j.cbi.2018.03.015.